

SLAC-PUB-4517
AP Note 62
January 1988
(A)

Results from the SLAC Lasertron*

J. J. WELCH[†]

*Stanford Linear Accelerator Center
Stanford University, Stanford, California, 94305*

ABSTRACT

Rf power at 2856 MHz has been obtained from the SLAC proof of principle lasertron. Experiments show that the electron beam is well bunched when the laser beam is well dispersed, the voltage high, and the current density low. However, if any of these criteria is not met, space charge forces can cause significant debunching. The maximum beam power to rf power conversion efficiency was 12.3%, and the maximum rf power was 2 kW. Both maxima were obtained under the same operating conditions, at a beam voltage of 75 kV. When the maximum efficiency was obtained, it was limited by the poor match of the beam impedance to the cavity impedance. The rf measurements, the technical problems that limit available current and voltage, and the theory of the coupling between the beam and the cavity are discussed.

To Be Submitted

*Work supported by the Department of Energy, contract DE-AC03-76SF00515.

[†]Present address: Wilson Laboratory, Cornell University, Ithaca, NY 14853.

1. Experimental Results

1.1 INTRODUCTION

The SLAC lasertron is a 'proof of principle' device designed to produce high efficiency, high rf power with the goal of providing the rf power source for the next generation of linear colliders. The 'principle' is that a suitably bunched beam, necessary for rf production, can be formed directly from a photocathode by short optical pulses repeated at the rf frequency. The basic design^{1,2} and simulation results³ have been described elsewhere.

1.2 DESCRIPTION OF EXPERIMENT

A high voltage DC supply is connected to a high voltage, ultra high vacuum tube by a coaxial cable which also stores energy for the beam pulse. A laser provides 50 ps optical pulses at a repetition frequency of 2856 MHz for about 1 μ s. The optical pulses are converted to current pulses by a GaAs photocathode located on the end of the high voltage electrode. The current pulses are accelerated and pass through a resonant cavity which is coupled to a load, and are absorbed in a electrically isolated tube called the collector (see Fig. 1).

1.3 RF POWER AND EFFICIENCY

The rf power is measured using a directional coupler in series with the load and either an rf peak power meter or an rf average power meter. The beam power to rf power conversion efficiency is determined by dividing the rf power by the applied voltage multiplied by the collector current averaged over the rf pulse. This will not be the true efficiency if part of the beam passes through the cavity but is scraped off on the drift tube before it reaches the collector. The rf

power was measured for various voltages and under different conditions, such as varied beam current, different positions of the laser spot on the cathode, varied intensity of the laser, and different mode locker tuning. In Fig. 2 are the first measurements of rf power, taken on 11/6/87. The rf power rises more or less linearly with applied voltage except below about 20 kV where it is somewhat depressed. The efficiency rises rapidly with voltage until about 20 kV, where it is more or less constant at 1%.

The theoretical limits on the rf power, efficiency and current are also plotted in Fig. 2. Individual points are computed for various voltages using the value of the collector current measured at that voltage, and then joined to aid the eye. The collector current was held approximately constant during each of the data taking runs, though typically it increased with voltage.

The theory is discussed in detail in the next section. The fundamental assumptions are:

1. The true beam can be represented by a constant velocity beam traversing the cavity at a constant radius.
2. I_{RF} , the fourier component of the current at the cavity resonant frequency, has a phase that maximizes the rf power production.

Note that there are no assumptions regarding space charge debunching, beam loading, dissipation, emission time uncertainty, or nonlinear dynamical effects. Such effects might show up as discrepancies between the theoretical limits and experimental values.

When the theoretical rf power is plotted as a function of voltage, it represents the rf power that would be expected if the bunching exactly matched the laser beam pulse train. This is taken to be an infinite train of 50 ps full-width, half-maximum Gaussian pulses. Since the transverse profile of the current density is not well-known, the theory can only provide limits based on minimum and maximum coupling. The actual value of the power should lie within those limits.

When the ratio of I_{RF} to the collector current I_{DC} is plotted against voltage, it represents the fractional rf current that is needed to explain the observed power levels, given the measured cavity parameters. It also depends on the transverse beam profile and is plotted for minimum and maximum radii, and defines the theoretical limits on the rf current. There is a further constraint that the fractional rf current must be between zero and two, which is a consequence of the implicit assumption that the current is quasiperiodic. Values of I_{RF}/I_{DC} above two imply that the amount of rf current needed to produce the observed rf power exceeds what is theoretically possible with delta function bunching of the collector current, assuming the current is located at the radius specified.

There appears to be no glaring inconsistency between the data and the theoretical limits in Fig. 2, but the limits are quite wide. However, the data at low voltage indicates the majority of rf was produced by beam close to $r = 0$, while the data at higher voltage indicates the majority came from beam near the edge of the drift tube at $r = 1$ cm. If the actual transverse beam profile was more or less constant during the run, then to explain the data one is forced into looking for a mechanism that effectively suppresses the rf current at low voltage, in this case below 20 kV, and allows almost perfect bunching at voltages above 20 kV. Space charge debunching is an obvious candidate. Another candidate is the

response time of the emission of electrons from GaAs. This response time is in part due to the finite transit time of electrons from the depth where a photon is absorbed to the surface. This transit time increases when the applied electric field is reduced since the absorption depth is constant. By decreasing the electric field one eventually makes the range in the transit times which correspond to the range in absorption depths, comparable with the rf period and the bunching is lost. This effect is independent of the current density, and depends only on the electric field and possibly the sample of GaAs.

The run on 11/6/87 was followed by another run on 11/9/87 with basically the same configuration except the cathode quantum efficiency was lower and the transition from the waveguide to the load was improved. The results from 11/9/87 are plotted in Fig. 3. The data resembles that of 11/6/87 in form: the power seems to be a linear function of voltage and the efficiency starts to level off at 1% above 20 kV. Again, one would suppose, based on the theory, that there is some mechanism that suppresses the rf current at low voltage. At higher voltages, both the power and the efficiency exceed what is theoretically possible with perfect bunching. The most likely explanation for this is that some of the current passing through the cavity is scraped off on the drift tube before it reaches the collector. The result is that the true beam power is underestimated. The 11/6/87 data may suffer from the same problem.

It became clear that because of the low beam currents, the cavity Q was too small for the retarding fields in the cavity to build up sufficiently to efficiently extract energy from the beam. A slide screw tuner was installed between the load and the cavity with the idea of boosting the Q . The slide screw tuner provides two degrees of freedom with which one can vary the magnitude and phase of the

reflection coefficient seen by the cavity at the position of the screw. Thus it is possible to increase the Q without changing the resonant frequency. In practice the position and depth of the screw were adjusted for maximum rf power on the peak power meter. Only one maximum was obtainable.

A run was made on 11/10/87 with collector currents about the same as during the 11/6/87 run, but with the slide screw tuner in place. The results are given in Fig. 4. The theoretical points are not given because the rf properties of the cavity slide screw tuner system were not measured. As anticipated, the slide screw tuner boosted the rf power and efficiency considerably, with efficiency of nearly three percent at voltages above 30 kV. However, the shape of the efficiency versus voltage curve was very similar to that in the first two runs. When the slide screw tuner was removed, the efficiency dropped back near the one percent level as shown in Fig. 5. It should be kept in mind that the transverse profile of the beam was not necessarily the same from run to run.

Following a cathode cleaning/activation cycle, higher currents were obtained for a series of runs made on 11/17/87. Also, a change was made to the optics which transports the laser beam to the cathode, making it possible to vary the spot size and position and observe it on an image of the cathode. An iris diaphragm placed at the cathode image could then be used to insure that no light produced current that would hit drift tube. All of the data taken on 11/17/87 is displayed in Figs. 6 and 7. The theoretical limits are omitted for clarity. The first set of data, (167 mA), used a laser spot which was about as big as the cathode. Further enlargement of the spot caused the collector current to go down substantially. The rf power, shown in Fig. 6, was about an order of magnitude more than that obtained in earlier runs, mainly due to the higher current.

The efficiency, shown in Fig. 7, is quite low though it is increasing rapidly with voltage. It does not level off with higher voltages the way it had in previous runs. After this data had been taken the laser was observed to be out of tune and the mode locker frequency was adjusted. Tuning the laser caused the current, rf power and efficiency to increase. Under these conditions the efficiency was substantially higher, particularly at lower voltages, though it is still less than one percent. These data (189 mA) are plotted in Fig. 8 with the theoretical limits. Unlike earlier runs, power and efficiency are far below the theoretical constraints. The fractional rf current appears to be increasing with voltage toward a modest value between 0.7 and 1.1 at 50 kV, but is much smaller at lower voltages.

The next data, in Figs. 6 and 7, (204 mA), was obtained after adjusting the optical beam size and position to get the most collector current. The mode locker frequency was also tweaked to give more stable laser beam. The maximum voltage was increased and there is perhaps an indication that the efficiency is nearing its maximum.

Readjustment of the optics to give the maximum rf power was made before the next data set (241 mA) was taken. The collector current was higher due to a steady increase in the laser power as the laser warmed up. The power is substantially higher than in the previous data set, but the efficiency is about the same. The efficiency is clearly reaching a maximum around 55 kV of 1.4%.

Without changing the position of the center of the optical beam spot, the beam size was reduced to a few mm or less by focusing (230 mA). The collector current went down slightly, while the power and efficiency went down by almost a factor of two. Furthermore, the efficiency did not level off even at voltages as high as 75 kV. The next data set (304 mA) was taken with the same conditions

as obtained before the beam was focussed, except the current was slightly higher. This data very closely resembled that of (241 mA) except the power is somewhat higher. Finally, an aperture was put in front of the laser beam to reduce the collector current to about one tenth its previous value. The efficiency dropped to the lowest levels obtained so far, possibly leveling off around 0.3%.

The data from the last two runs, (304 mA and 32 mA), are plotted in Figs. 9 and 10. Just as in (189 mA), the experimental data lies well below the theoretical constraints, for both runs. The rf current is suppressed substantially, but I_{RF}/I_{DC} appears to be leveling off to somewhat below one in both cases. This would seem to indicate that at least some of the inefficiency is not due to space charge debunching, since that effect would cause I_{RF}/I_{DC} to increase with voltage, until it reached 1.86, the value corresponding to for 50 ps current pulses. The current density at the cathode was not changed between the two runs, except that it went to zero over a large region. The spot size appeared to the eye to be about 4 mm in diameter when the aperture was restricting the current. This implies current densities must have been above 0.24 A/cm^2 possibly an order of magnitude greater.

There are several reasons to believe that the suppression of rf current evident in Figs. 6 through 10 is due largely to space charge debunching. All figures show that the true rf current must decrease as the voltage is lowered, at least for voltages above about 20 kV. Comparing the plots of I_{RF}/I_{DC} versus voltage in these figures with that in Fig. 2, where the current density is about an order of magnitude lower, shows the suppression is much greater when the current density is greater. Also, when the beam was focussed the suppression is clearly greater. The suppression does not depend very much on the total current, as it might if

there were nonlinear dynamical effects due to beam loading. This can be seen in Fig. 10 where the current density is the same but the total current only one tenth that in Fig. 9. Furthermore, rough estimates of debunching due to space charge indicate that space charge debunching occurs if the optical beam is concentrated to a one centimeter or smaller spot on the cathode. Such concentration is plausible given the spot was made up from eight separate beams, each of which delivers its light at a different time from the others. Below 20 kV, the suppression of rf current could be due to emission time uncertainty.

In an effort to get higher power and efficiency with the same cathode and laser power, the slide screw tuner was reinstalled. The data obtained is shown in Fig. 11. At voltages below about 45 kV the efficiency resembles that obtained without the slide screw tuner. Rather sharply, around 45 kV, the efficiency rises to almost 6% and the power rises to nearly 800 watts at 85 kV. The collector current increases only slightly with voltage and there is no rapid change observed corresponding to the change in the rf power.

All of the previous results were obtained with a rather peculiar laser pulse train. Streak camera photos (see Fig. 12) and Tektronix 7104 traces using a very fast photodiode (≤ 35 ps risetime) both show very strong amplitude modulation of the pulse train. The modulation amplitude is typically as large as the average pulse height and is not constant within each 1 μ s rf pulse, nor is it constant from rf pulse to rf pulse. They also show that the spacing between individual pulses is not accurately one rf period, and varies in phase by as much as 120 degrees. Some of the variation is periodic at one eighth the rf frequency, indicating the legs of the multiplexer were not quite at the correct length, but most of the variation was erratic. It turned out that the problem is generic to mode locked lasers and

is discussed in more detail later in this paper. This problem was corrected and the laser pulse train was stable during collection of the data that follows.

In order to reduce the possibility of high current density spots on the cathode, the laser beam was defocussed until about one half of the initial collector current remained. The laser spot appeared to be round, although there were several ancillary spots near the bright spot that was directed to the cathode. An adjustable aperture, on the cathode image fixed the maximum beam diameter at 21 mm. This technique effectively eliminates current that might scrape off on the drift tube. A microwave average power meter was used for some of the following data and the peak power was inferred by dividing the reading by the duty cycle.

With the changes mentioned above made, the rf power and efficiency were measured and the results are shown in Fig. 13. Note that the slide screw tuner was not used in this measurement. As usual the rf power starts around 10 or 20 kV and rises linearly until about 50 kV. The efficiency rises to a relatively high value of 3%, flattens out and then starts to drop with voltage. The drop is expected to occur if the rf current in the cavity is not increasing with voltage, because for a fixed rf current the cavity voltage is fixed and therefore a smaller fraction of the beam energy is extracted. Another run was taken under almost the same conditions using a peak power meter. The results are shown in Fig. 14. The general features are the same, though the efficiency is not quite as high nor is the plateau in rf power clearly evident. The suddenness of the drop in the efficiency around 55 kV in Fig. 13 does not appear in Fig. 14, and is probably due to drift in the laser power and position.

As the voltage is increased, it is somewhat surprising to see in Figs. 13 and 14, the efficiency approach the lower theoretical limit from above. However, the

detailed shape of efficiency versus voltage depends on the actual beam profile. At low voltages, beam from larger radii may contribute the most to the rf power. When the voltage is raised, the ratio of the coupling for $r = 1$ to $r = 0$ becomes smaller, and the relative contribution from current near $r = 0$ increases. If most but not all of the current is from near $r = 0$, then one would expect the efficiency to drop slightly faster than the theoretical efficiency at constant radius.

From the two figures it is clear that the fractional rf current must be between about 1.33 and 1.83. The theoretical value for the measured laser pulse train with 50 ps pulses is 1.86. The pulse width that corresponds to the lower limit, is 119 ps.

A series of neutral density filters were placed in the laser beam which reduce the laser intensity without changing the spatial or temporal profile. The collector current was found to be proportional to the factory calibrated transmission values for each filter. In theory, if the rf current is proportional to the collector current, the power should be proportional to the collector current squared. The best fit square law is drawn for each set of points, $r = 0, 0.5$ and 1.0 cm in Fig. 15, and shows no inconsistency with the constant proportionality assumption. The average power meter data shown in Fig. 15 indicates the data is almost exactly the same as the theoretical points for $r = 0$. The data from the peak power meter more closely agrees with the curve for $r = 0.5$. The difference is probably due to a drift in the laser spot position or mode locker tuning. If space charge effects were present, then one should expect the rf power to increase less rapidly than the square of the collector current. So one may conclude that at 75 kV with a current at least 44 mA/cm^2 , that space debunching is negligible.

At this point the slide screw tuner was installed and optimized to give an rf power of 1.04 kW and an efficiency of 9.5%. Then the laser focussing was adjusted again to give the maximum rf power and the slide screw tuner readjusted. The laser spot appeared not to have changed. The power obtained, still at 75 kV, was 2.07 kW with an efficiency of 12.3%. The rf waveform envelope showed that the loaded Q was approximately 3500. This is the same Q as found previously for much smaller currents and probably represents that maximum Q that can be reached with the slide screw tuner. Presumably, a higher Q would yield even higher efficiency.

1.4 LASER PERFORMANCE

The laser consists of a mode locked oscillator, an acousto-optic deflector, two optical amplifiers, a frequency doubler, and an 8X pulse multiplier. The oscillator makes 75 ps pulses (full width half maximum) at a frequency of 357 MHz of 1.06 μm wavelength light. A 1 μs portion of the oscillator beam is deflected out by the acousto-optic deflector 60 times a second. The deflected beam is sent through two optical amplifiers, which boosts the pulse to its maximum power. There is one stage of optical isolation between the two amplifiers which is done using a Faraday rotator, polarizing beamsplitting cubes and a calcite polarizer. After amplification, the pulses are converted to 530 nm light by a KTP frequency doubler; it also shortens the pulses to about 50 ps. Finally each pulse is split into eight separate beams which are recombined at variable delays to bring the pulse frequency up to 2856 MHz.

A similar laser was built for a lasertron being developed at KEK.⁴ Both the SLAC and the KEK laser use the so called MOPA design, (master oscillator power

amplifier), in which a short burst of pulses from a mode locked oscillator is sent into a high gain amplifier chain. The main differences are the SLAC laser lacks a third stage of amplification and its associated optical isolator, the SLAC laser oscillator operates at 357 MHz ($1/8$ of the rf frequency) rather than 178.5 MHz in the KEK laser, and the KEK laser has a gain compensating 'waveform shaper' while there is no compensation for the drop in gain during the rf pulse in the SLAC laser.

The laser output may be described in terms of the optical power, pulse to pulse amplitude stability, pulse to pulse temporal stability, and transverse spatial profile and stability. There may also be a CW component in addition to the 50 ps pulses.

Initially the pulse multiplier was bypassed and the temporal behavior of the 357 MHz beam was observed on a IMACON 500 streak camera. A somewhat better than typical trace is shown in Fig. 12. Evident is a strong amplitude modulation at roughly one third of the pulse frequency. There are also fluctuations in the temporal spacing of the peaks with an rms of about 60 ps. Some traces show additional peaks halfway in between the 'regular' pulses. The pulse widths varied but were in the range of 35 to 90 ps.

It was found that the poor pulse to pulse characteristics were due to the presence of multiple transverse modes in the oscillator. These modes oscillate at slightly different optical frequencies and consequently causes beating effects between the axial modes associated with them. The relative amplitudes of different transverse modes are not constant in time and depend sensitively on the relative loss and gain in the oscillator cavity. By reducing the aperture in the oscillator it is possible to ensure that only the skinniest mode has small enough loss

to oscillate. When this was done the pulse to pulse amplitude stability improved dramatically. However, the output power dropped by about a factor of ten.

The pulse to pulse spacing is set by the length of the delay legs in the pulse multiplier. Using the streak camera it possible to set these delays to within about 10 ps of the appropriate value.

The streak camera also showed a shifted noise baseline, but it may not be representative of a CW component in the beam. A shift in the noise baseline occurs even if the streak camera is triggered after the laser pulse is over, provided the delay is not too long. In this case, there is no doubt that it is streak camera generated. In theory, the intensity of the optical pulse train at the oscillator is approximately proportional to

$$\frac{\sin^2\left(\frac{N_{max}\Delta\omega t}{2}\right)}{\sin^2\left(\frac{\Delta\omega t}{2}\right)},$$

where N_{max} is the number of axial modes that are oscillating (it is assumed with equal amplitude) and $\Delta\omega$ is 2π times the frequency spacing between axial modes. The intensity is large whenever the denominator goes through zero; that is, every cavity round trip period $T \approx 2.8$ ns. The width of each pulse is measured at 75 ps $\approx T/N_{max}$, thus N_{max} is about 37. One should then expect smaller peaks to appear with the frequency of $\pi N_{max}\Delta\omega$ and with peak heights $\geq 1/N_{max}^2$ of the main peak height. When the pulses go through the frequency doubler, because the doubling efficiency depends on the square of the electric field amplitude (within limits), the main peak is emphasize even more.

The laser power was substantially below the original design. The output from the mode locked oscillator was about 0.7 watts. Only about 12 to 15% of

this was deflected into the amplifier chain for the 1 μ s rf pulse. The net gain in the amplifier sections, including loss due to the optical isolator, was less than or equal to 8500, which gives about 77 mW or less average power at the frequency doubler. The efficiency of the frequency doubler was less than or equal to 5%, mainly due to the fact that the optics were optimized for higher power beams. The power was reduced by about another factor of ten in the multiplexer. This was due to difficulties in alignment and drift of the beamsplitter transmission angle with time. The beamsplitters were thin film beamsplitters manufactured by CVI and must be set at very close to the correct angle in order to cleanly split the beam into two polarizations. Unfortunately, because the coated surfaces that do the splitting are exposed to environment, they can adsorb moisture and the optimal transmission angle changes with time. Consequently, all the downstream alignment has to change. At times, the multiplexer efficiency has been as high as about 65%. The net result after the multiplexer, is that a typical average laser power is about 0.3 mW. With the existing equipment, it probably possible to get this up a few milliwatts. The original design called for about 1 W of average laser power.

1.5 HIGH VOLTAGE AND CATHODE PERFORMANCE

The high voltage capability of the system was intimately linked to the activation of the cathode. With a fresh cathode and either new or freshly polished electrodes, the tube processed to the maximum available voltage 400 kV, with field emission currents of a few microamperes or less. The peak electric field occurred on the cathode electrode and was 14.7 MV/m at 400 kV. After a cathode had been activated, by exposure to cesium and NF_3 , the high voltage behavior

changed dramatically. There appeared large field emission currents, (> 1 mA at 60 kV), which turned on and off randomly. Coupled with the large currents were increases in the system pressure. When the tube was in a high current mode, the lifetime of activated photocathode could be as short as a few minutes. Sometimes the large emission currents could be reduced by keeping the high voltage on for many hours or days, but not without a complete loss of cathode quantum efficiency. The highest voltage obtained with an activated cathode was about 100 kV. This voltage was only maintained about one hour before a vacuum arc occurred and the cathode activation was lost, essentially instantaneously.

It was found that the large field emission currents originated from the vacuum melted 316 stainless steel cathode electrode, near but not at the highest field points. Several deep holes were melted into the anode opposite the emission sites. The GaAs, on the other hand, showed no large field emission behavior. Current from the GaAs photocathode was confined by the magnetic field and reached the collector. Typically, the collector current was only a few picoamperes. SEM analysis showed that large quantities (many monolayers) of cesium had been deposited on the cathode electrode. It is reasonable to suppose that similar quantities occurred on the anode as well given the geometry of the cesiator.

2. Analysis

In order to understand the experimental results it is necessary to calculate, in some detail, the expected performance of the cavity for relevant beam voltage and currents. I used Urmel to generate the approximate electromagnetic fields assuming no coupling to a load. The Urmel calculation yields the following results:

$$U_0 = 0.178 \times 10^{-5} \text{ joules of stored energy ,}$$

$$Q_0 = 6834 \text{ is the uncoupled } Q \text{ ,}$$

$$V_0 = \sqrt{\int E_{z_0} \cos\left(\frac{kz}{\beta}\right)^2 + \int E_{z_0} \sin\left(\frac{kz}{\beta}\right)^2} \text{ ,}$$

where E_{z_0} is the electric field in the axial direction, $k = \omega/c$ where ω is the resonant angular frequency of the rf cavity, $\beta = v/c$ where v is the velocity of the electrons in the beam and c is the velocity of light. The quantity V_0 depends on both energy and path. If an electron travels parallel to the axis at constant speed, then V_0 is the maximum energy gain or loss with respect to rf phase.

I will calculate the rf power that will be obtained for a given rf current, and conversely, the rf current necessary to generate the observed power. I assume the rf power may be written as

$$P_{RF} = \frac{1}{2} I_{RF} V(r)$$

where $V(r)$ has the same definition as V_0 except the URMEL generated fields are replaced by the true cavity fields. I_{RF} is the Fourier component of the current in the cavity at the resonant frequency of the cavity, $\int e^{i\omega t} I(t) dt$

The correct expression for the rf power is

$$P_{RF} = \text{Real} \left\{ \frac{1}{2} \int d^3x \tilde{J}^*(x, \omega) \cdot \tilde{E}(x, \omega) \right\}$$

where $\tilde{J}^*(x, \omega)$ is the complex conjugate of the temporal fourier transform of the current density, and $\tilde{E}(x, \omega)$ the temporal fourier transform of the electric field. If one assumes that all electrons follow the same trajectory at the same constant speed, that the rf current has a phase such that a maximum amount of energy is extracted from the electrons by the cavity fields, and there is no dissipation, then the integral expression reduces to the simplified expression for power. The above approximations of constant speed and straight line trajectory are probably good because little energy is extracted from the lasertron electron beam. The current however, is not confined to a particular radius. As we shall see, the variation of $V(r)$ with r has a significant effect on the estimate of the relation between power and current. The approximation that there is no dissipation is also good since $Q_0 \gg Q_L$, where Q_L is the measured Q of the cavity when connected to a matched load.

Ignoring dissipation, $Q_L = \omega U / P_{RF}$. In steady state, the rf power delivered to the load by the fields in the cavity must be equal to the power extracted from the beam.

$$\frac{1}{2} I_{RF} V(r) = \frac{\omega U}{Q_L} = P_{RF} .$$

Using URMEL to relate U and $V(r)$,

$$\frac{U}{U_0} = \frac{V^2(r)}{V_0^2(r)} ,$$

we arrive at

$$P_{RF} = \left(\frac{Q_L}{\omega U_0} \right) \left[\frac{V_0(r)}{2} I_{RF} \right]^2 ,$$

$$I_{RF} = \left[\frac{2}{V_0(r)} \right] \sqrt{\left(\frac{\omega U_0}{Q_L} \right) P_{RF}} .$$

The rf current will be related to the collector current depending on how well bunched the electron beam is, assuming it is bunched at the resonant frequency and does not vary in time. For example, if the bunches had zero length, fourier decomposition yields $I_{RF}/I_{DC} = 2$. Similarly, if the beam was bunched with the same shape as the optical beam, that is with a 50 ps gaussian pulses, then $I_{RF}/I_{DC} = 1.86$.

The line integral $V_0(r)$ has been calculated for various beam energies and radial positions and the results are given in Fig. 16. At low voltage, where the transit time effect suppresses energy extraction, the ratio of $V_0(r = 1 \text{ cm})$ to $V_0(r = 0)$ is much larger than one. This means that the amount of energy it is possible to extract from the beam varies greatly depending on where the beam passes through the cavity. At higher voltage, the ratio is closer to one and variations in rf power due to path become less significant. Since the beam does not pass through the cavity at a single point, the appropriate weighted average of the beam current should be used to compute the correct rf current when estimating the rf power. I assume $V(r)$ is a monotonic function of r . Then the estimated rf current, obtained from the power measurement, must lie between curves corresponding to minimum and maximum V_0 ; that is between $V_0(r = 1 \text{ cm})$ and $V_0(r = 0)$. Of course, one has the additional constraint on I_{RF} that $I_{RF}/\langle I \rangle \leq 2$.

3. Conclusion

This work has demonstrated that at least a reasonably well-bunched beam can be produced in a lasertron, with a full width half maximum between 50 and 119 ps, which can generate rf power. The maximum observed rf power, 2 kW at 75 kV, was made with a beam power to rf power conversion efficiency of 12%. This efficiency was limited by the mismatch between the cavity impedance and the beam impedance. Higher currents would be needed improve the matching, but were not available due to lack of laser power.

The laser for the SLAC lasertron operates at far below the specified power levels, and with large amounts of 'noise' of various kinds. This is principally due to inadequate design, although faulty or 'worn out' parts are also partly to blame.⁵ The laser for the KEK lasertron has met or exceeded its design specifications. These specifications are consistent with the specifications for the SLAC lasertron laser except the repetition rate for the KEK laser is 5 Hz, versus 60 Hz for the SLAC laser.

It was shown by using neutral density filters, that space charge effects were not significant when the maximum rf power was obtained. But, in other runs, space charge effects had caused a large reduction in the fraction of beam current converted to rf current, particularly when the laser spot was concentrated. Thus space charge effects can reduce the rf current in the lasertron, which causes even more mismatch between the beam impedance and the cavity impedance. Given the limitations on the cavity Q and therefore the cavity impedance, in order to efficiently utilize a much higher current beam, the space charge effects will have to be overcome. Presumably, once the laser spot is spread out, the only way to do this is by raising the voltage. Unfortunately, application of higher voltages

caused large field emission currents and some arcing, and destroyed the cathode quantum efficiency.

The SLAC lasertron was designed to hold off 400 kV under the assumption the gap would behave much like that in a conventional electron gun or high power tube. In fact, after high voltage processing essentially virgin electrodes, the SLAC lasertron was able to hold off 400 kV for many hours. The high voltage conditioning was lost however, when the cathode was activated by exposing it to cesium and NF_3 . If the cathode was activated before high voltage processing, the activation was lost during the processing. In either case, the voltage at which a working cathode could be maintained was less than 100 kV DC.

The poor high voltage behavior of the SLAC lasertron appears to be due to excessive amounts of cesium deposited on the electrodes during cathode activation. In principle, this can be eliminated by shielding the electrodes, or collimating the cesium flow, or by first activating the cathode in a remote location and then moving it into place as is done in the KEK lasertron. However, the realization of very high voltage $\gtrsim 400$ kV activated photocathodes has not yet occurred.

Clearly, the lasertron has a long way to go before it could be useful as an rf source for the next generation of linear colliders. Various designs of linear colliders require sources from ~ 200 MW (together with pulse compression), to over 1 GW, with a substantially shorter wavelength than 10 cm used in the proof of principle experiment. The SLAC proof of principle device has attained 2 kW at 75 kV DC with 12% efficiency. The KEK lasertron has reached 80 kW at 150 kV pulsed voltage,⁶ with a maximum efficiency of 2.5%. Furthermore, after about three years of effort, neither the SLAC or KEK lasertron has come close to their designed operating points. On the other hand, no fundamental technical problems have been found.

REFERENCES

1. E. L. Garwin, W. B. Herrmannsfeldt, C. K. Sinclair, J. Weaver, J. J. Welch and P. B. Wilson, *An Experimental Program to Build a Multimewatt Lasertron for Super Linear Colliders*, Proc. of the 1985 IEEE Particle Accel. Conf., p. 2906; SLAC-PUB-4111 (1986).
2. C. K. Sinclair, Proc. of the 1986 Madison Accel. Sympos., p. 298; SLAC-PUB-3650 (1985).
3. J. J. Welch, *Beam Dynamics, Efficiency and Power of the SLAC Lasertron: Simulation Results*, Proc. of the 1986 Stanford Linear Accelerator Conf., p. 81; SLAC-PUB-3977 (1986).
4. H. Imoto *et al.*, Proc. from CLEO (1987).
5. The laser was designed and built by XMR of Santa Clara, California.
6. Tsumoru Shintake, personal communication.

FIGURE CAPTIONS

1. The experimental arrangement of the SLAC lasertron.
2. Rf power, efficiency and the ratio of rf current to the collector current are shown in separate plots. The data was obtained on 11/6/87 with a collector current of 31.5 mA at 50 kV. Theoretical limits based on the theory given in Section 2 are also plotted.
3. These are the data with a lower beam current and improved waveguide to load transition. Note that the power and efficiency exceed what is theoretically possible.
4. A slide screw tuner was installed to externally boost the cavity Q , presumably without changing the frequency. The collector current, 57 mA at 50 kV, is almost the same as that on 11/6/87 (Fig. 2), but the efficiency is almost a factor of three higher.
5. Here the slide screw tuner has been removed. The efficiency drops, but the lower bound on I_{RF}/I_{DC} is almost two at the highest voltage!
6. The slide screw tuner was not in place when the data for this figure was taken. A broad laser spot illuminated the cathode in '167 mA', then the laser mode locker frequency was retuned for '189 mA'. The data '204 mA' was obtained after adjusting the focus and position of the laser spot to obtain the maximum collector current. The optics were readjusted in '241 mA' to get the maximum rf power. Then without changing the position of the center of the spot, the beam was focussed in '230 mA'. The optics were again adjusted to maximize the rf power in '304 mA'. Finally, an

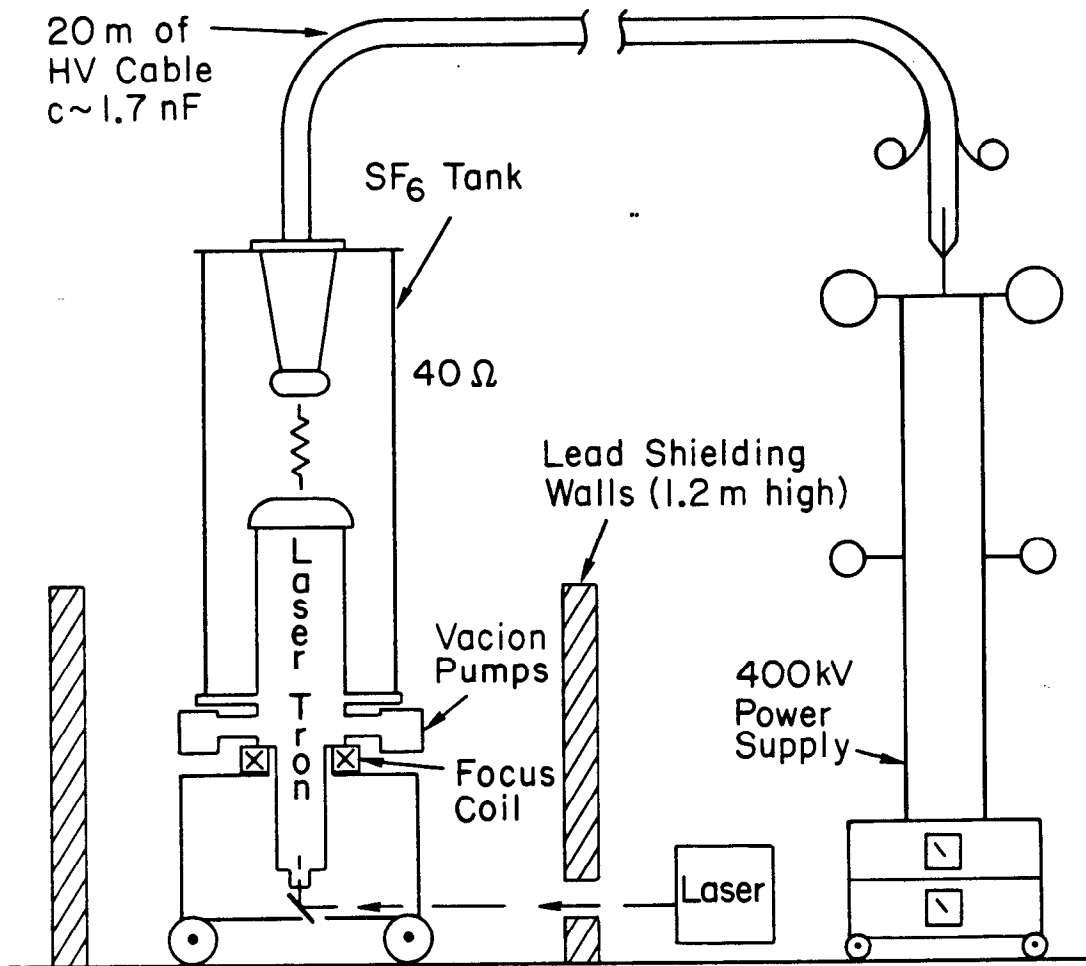
aperture blocking the laser beam was installed to lower the collector current in '32 mA'.

7. These results are computed from the same data as shown in Fig. 6.
8. This is the data obtained after the laser mode locker was retuned to give shorter, more stable laser pulses. The collector current was 189 mA at 50 kV.
9. Here optics were adjusted to give the maximum rf power. The current, 304 mA at 50 kV, was the highest ever obtained with the SLAC lasertron.
10. An adjustable circular aperture was installed to reduce the collector current to about one tenth its previous value.
11. The slide screw tuner was installed and adjusted to give the maximum rf power. The sharp rise in efficiency and power around 45 kV was accompanied by a change in envelope of the rf waveform, leading one to suspect that there may be some dramatic changes in the dynamics of the beam around 45 kV. The collector current was 148 mA at 50 kV.
12. This streak camera photograph shows the individual laser pulses before the $8\times$ multiplier. The erratic behavior is due to the simultaneous oscillation of more than one transverse mode in the CW oscillator.
13. The laser pulse train structure was greatly improved and the laser beam spot spread out to obtain this data. Even though the current is relatively high, the experimental points lie (barely) within the theoretical limits, rather than very much lower than the lower limit, as seen in the previous high current data. (See Figs. 8 and 9.)

14. The data here was taken with a peak power meter and in the reverse order from that of Fig. 13, and the results are substantially the same. At high voltage, the limits on the I_{RF}/I_{DC} imply that the bunching must be fairly good.
15. For this data the laser beam shape was kept constant in both space and time, and the current was varied by inserting neutral density filters in the laser beam. The two data sets shown differ only in the order in which the data was taken and the meter used to measure the power. The average power meter was used to collect data for the plot on the left, while the peak power meter was used to collect data on the right.
16. V_0 is the maximum voltage loss of an electron which travels parallel to the axis at constant velocity, with respect to rf phase. It is equal to

$$\sqrt{\int E_{z_0} \cos\left(\frac{kz}{\beta}\right)^2 + \int E_{z_0} \sin\left(\frac{kz}{\beta}\right)^2}.$$

The overall scale is determined by URMEL and is not related to any field values in the lasertron.



5-85

5054A5

Fig. 1

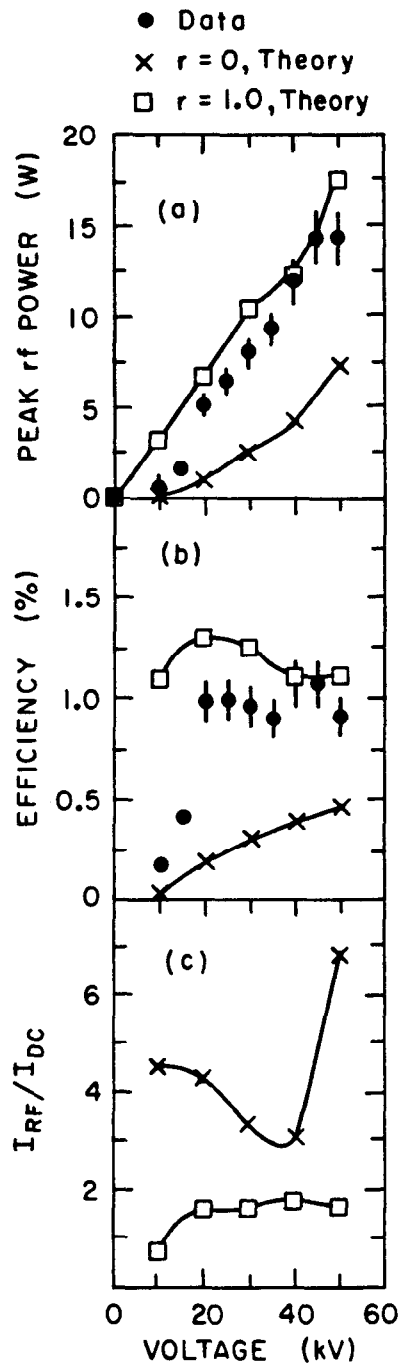
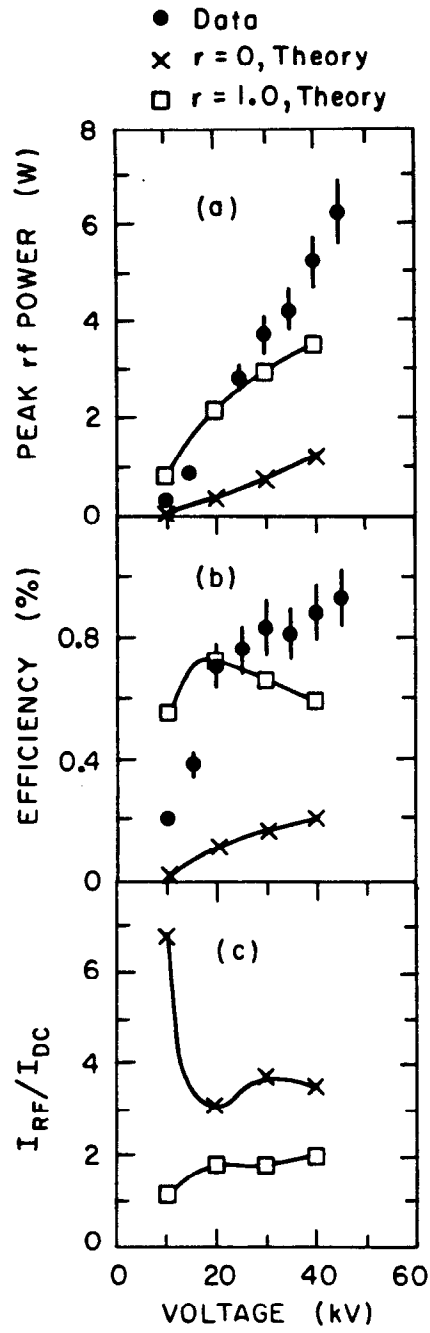


Fig. 2



1-88

5935A2

Fig. 3

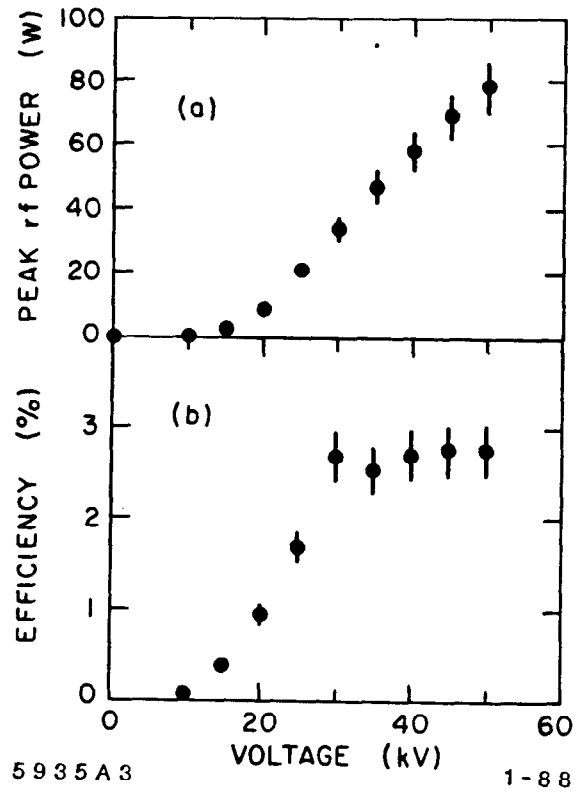
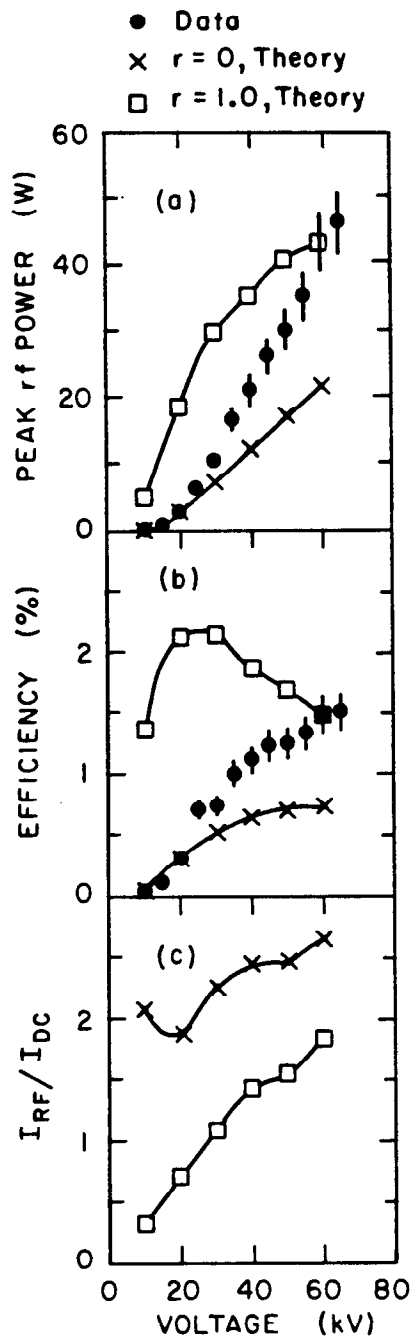


Fig. 4



1-88

5935A4

Fig. 5

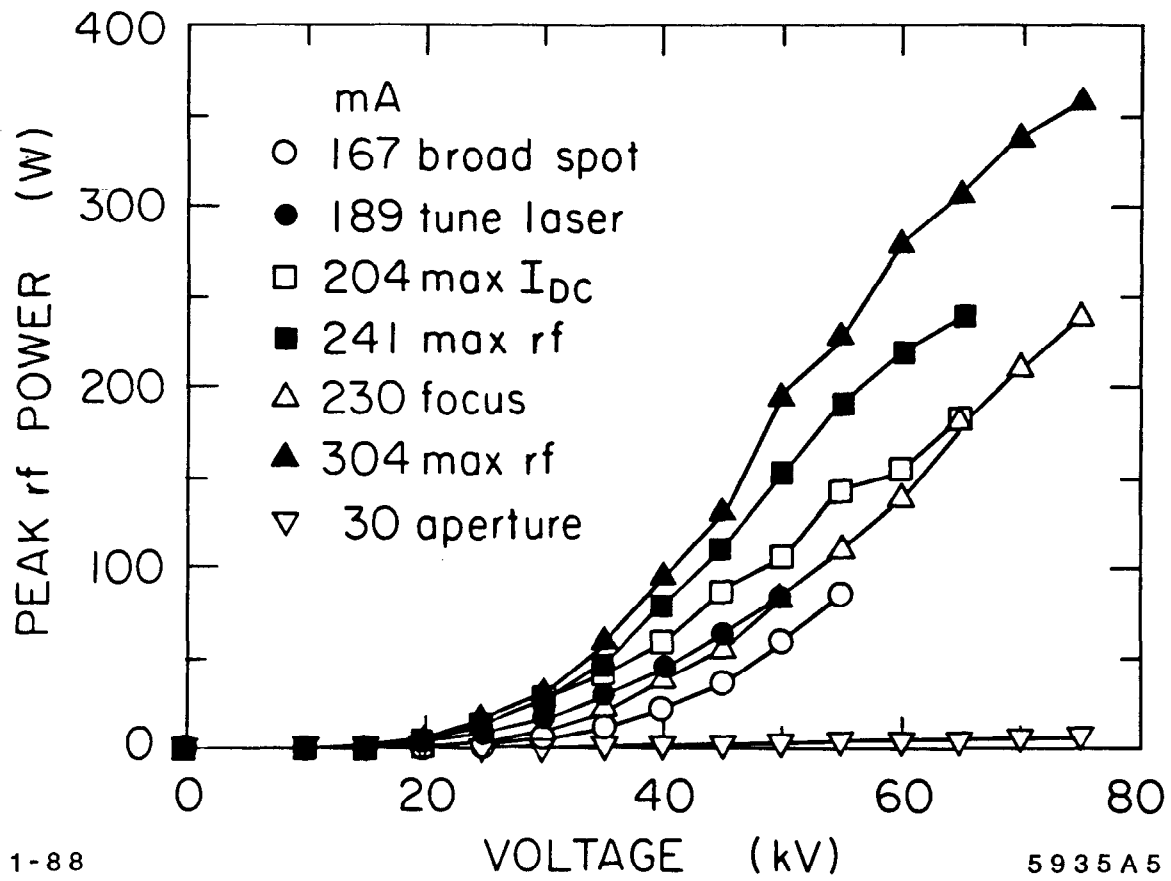


Fig. 6

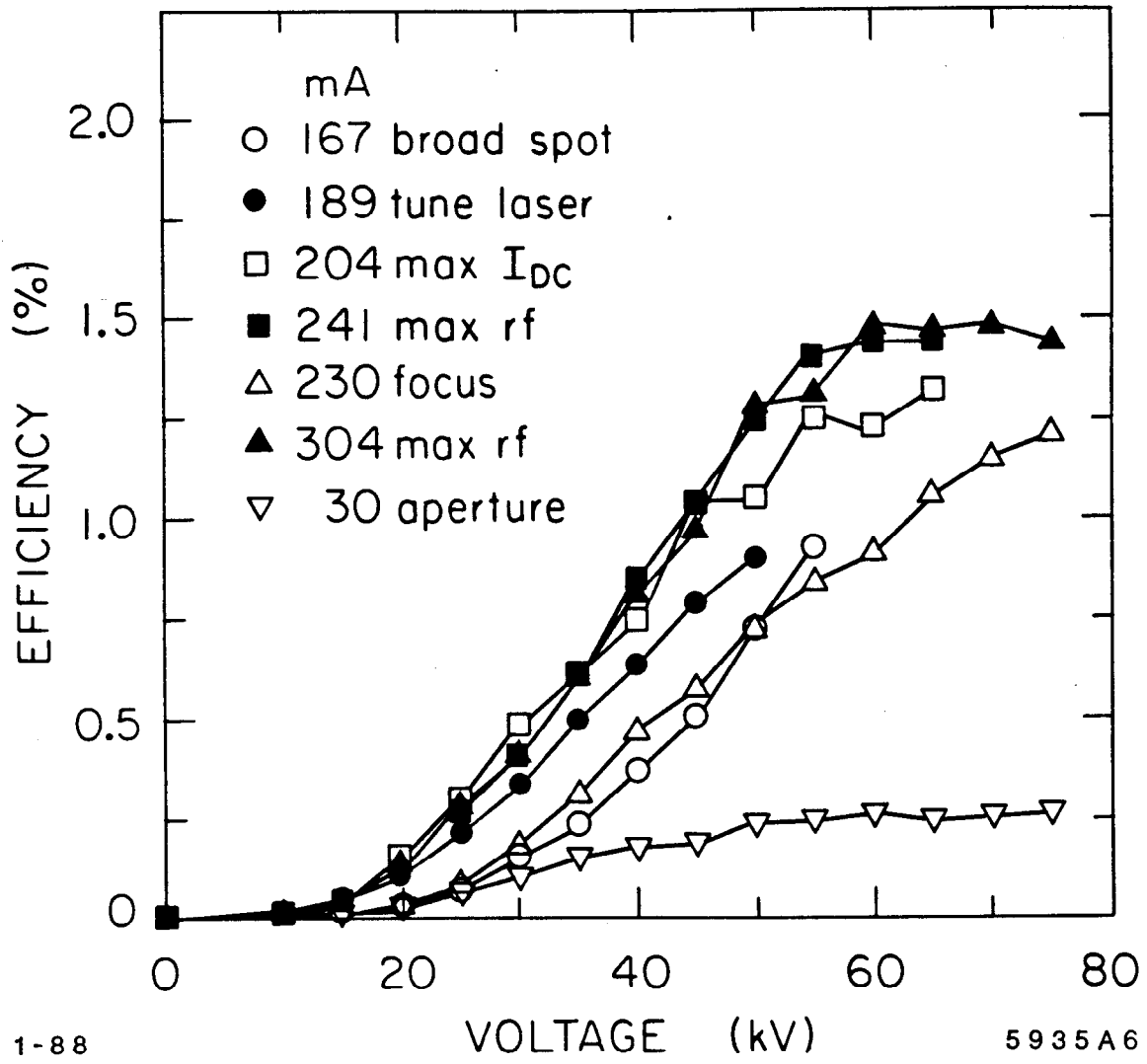


Fig. 7

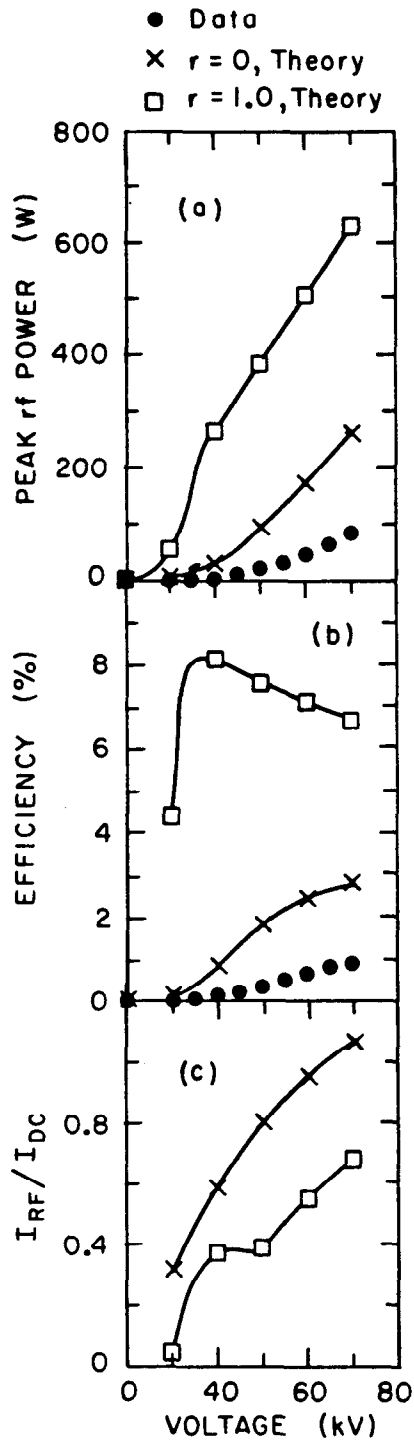
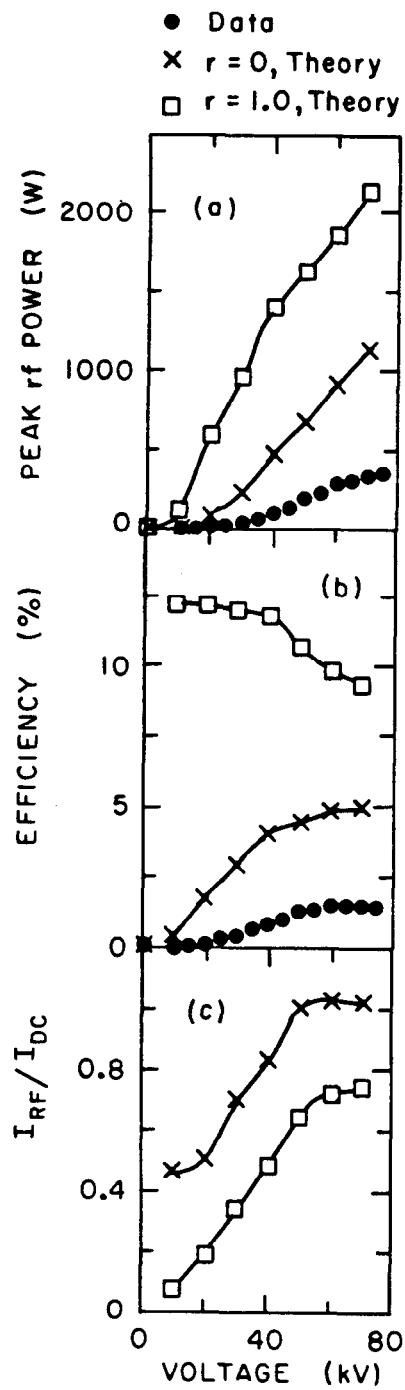


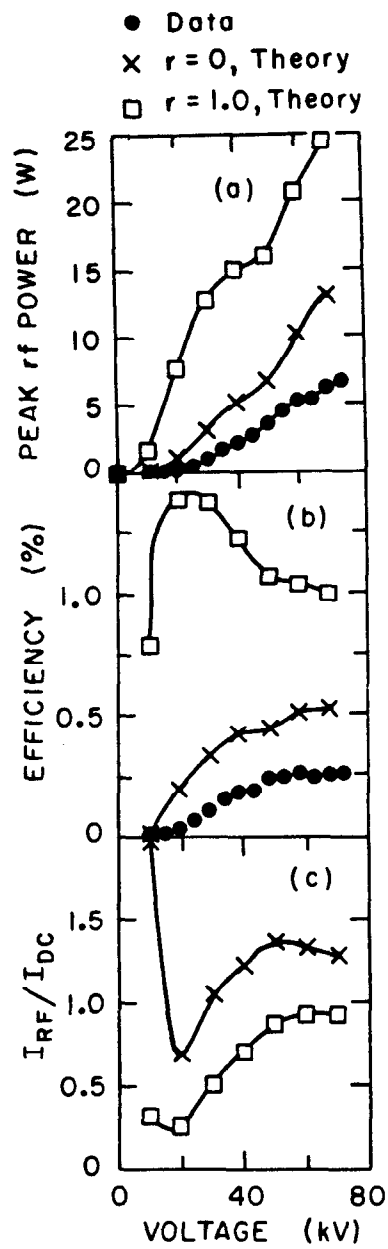
Fig. 8



1-88

5935A8

Fig. 9



1-88

5935A9

Fig. 10

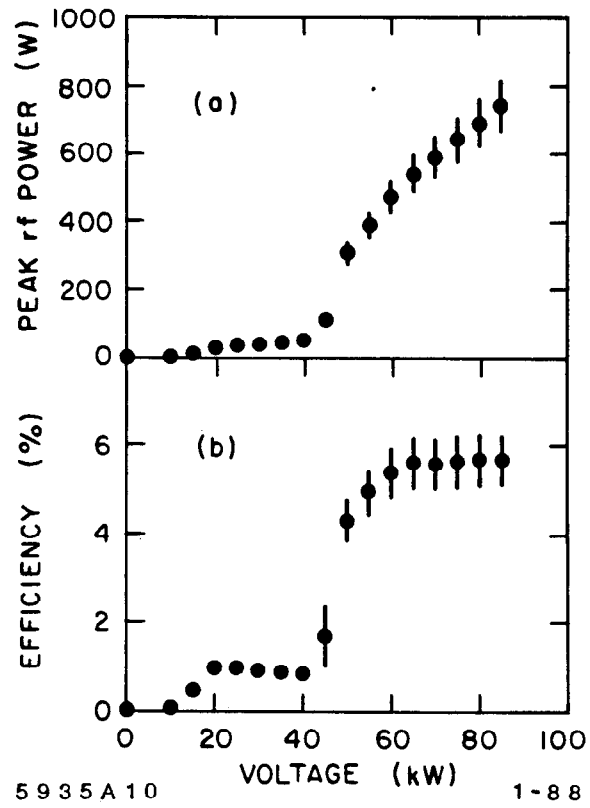
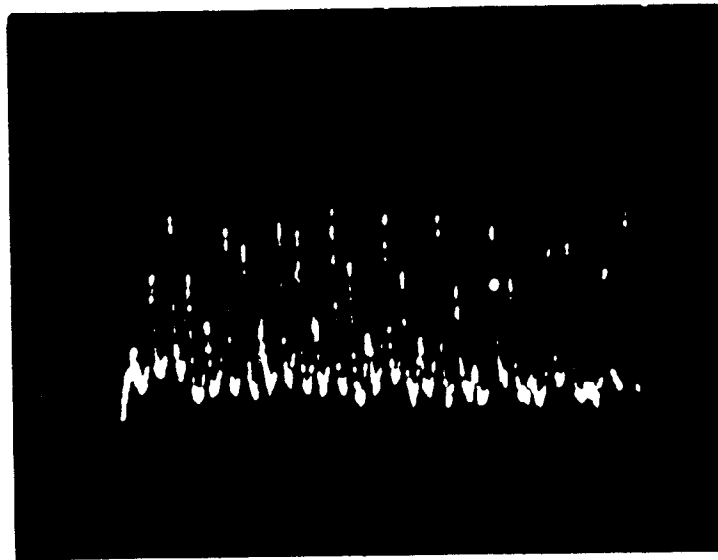


Fig. 11



1-88

5 nsec/mm

5935A16

Fig. 12

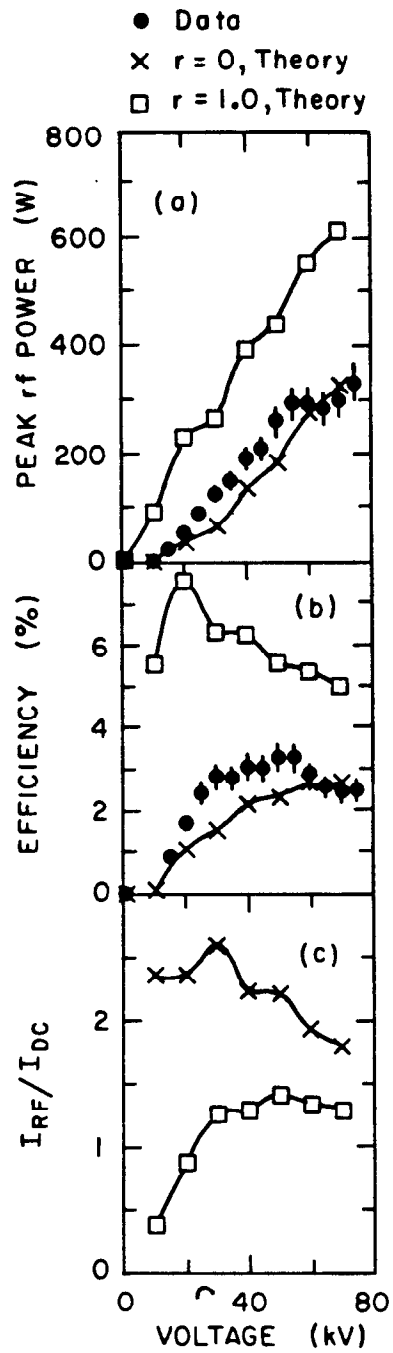
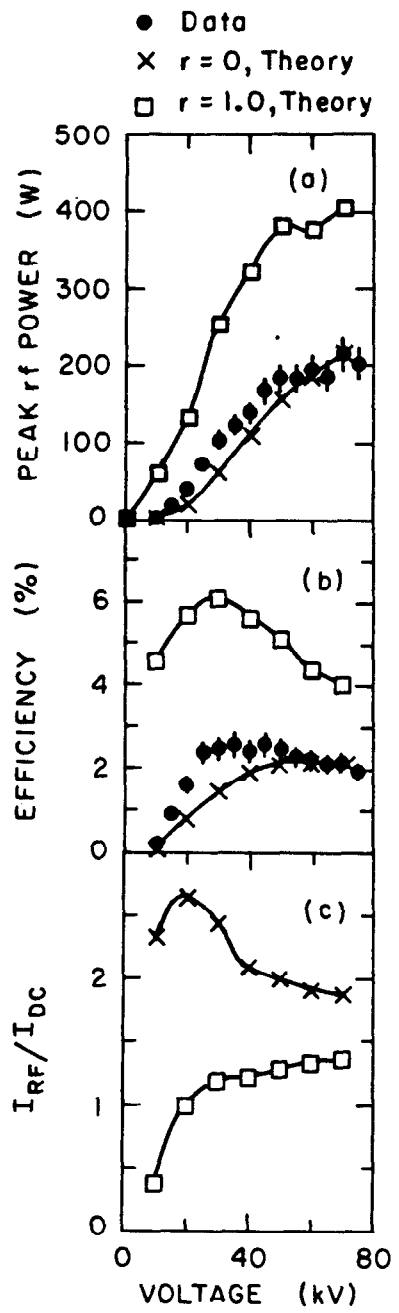


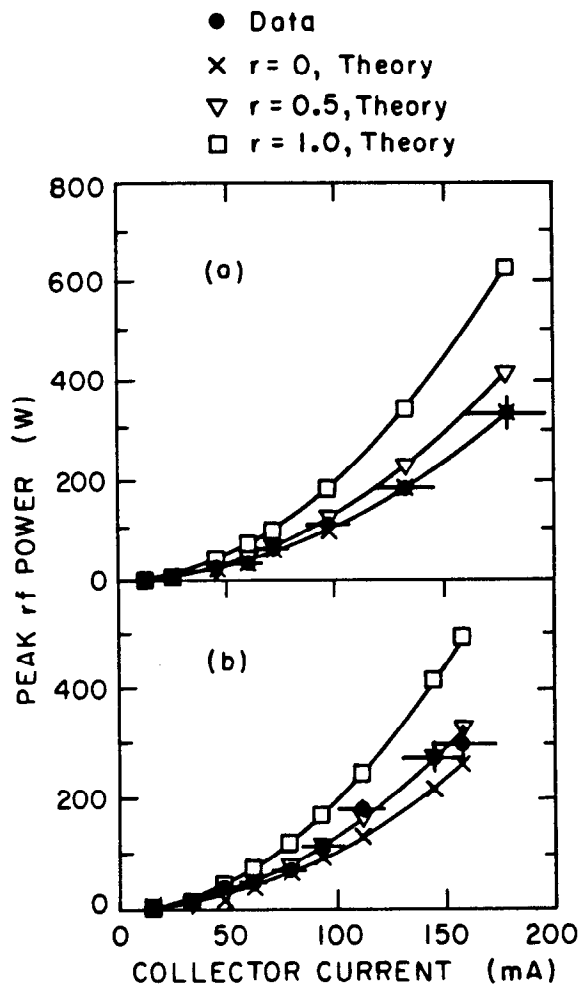
Fig. 13



1-88

5935A12

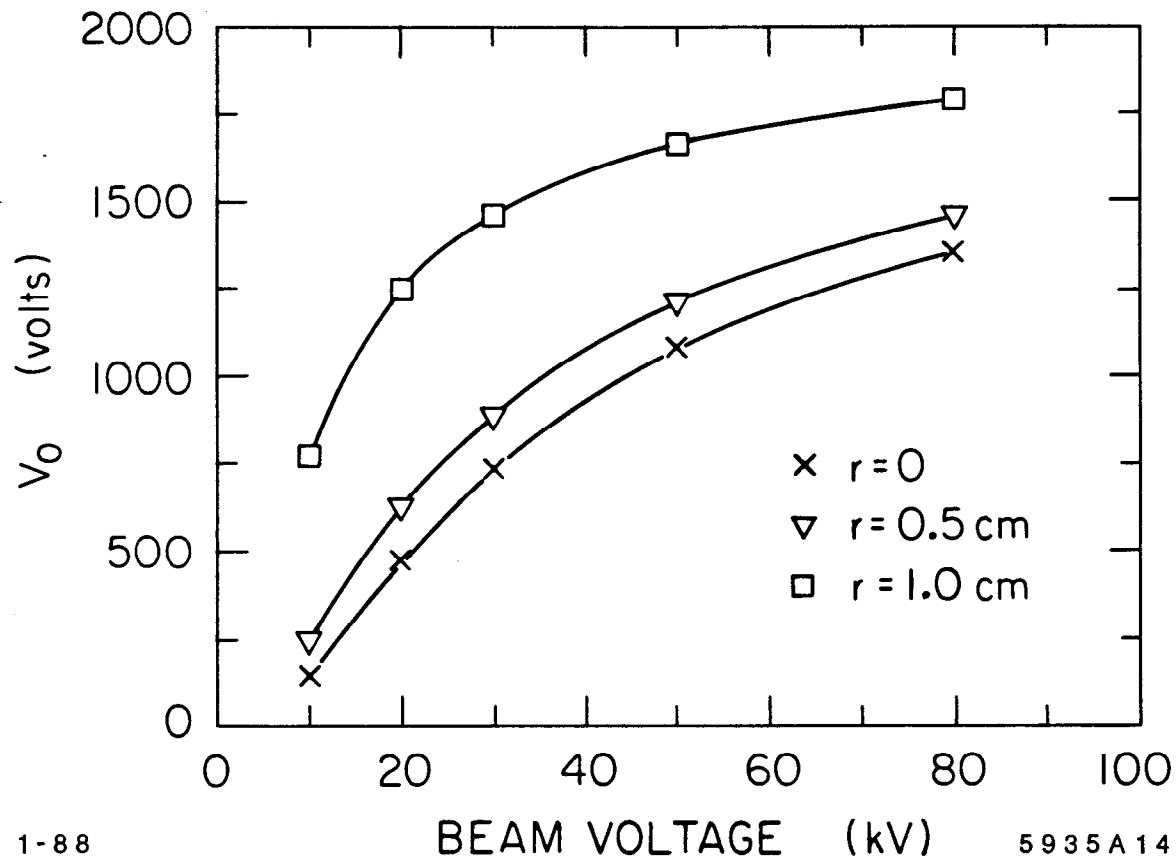
Fig. 14



1-88

5935A13

Fig. 15



1-88

5935A14

Fig. 16